Simple Analytic Solutions to Incompressible Irrotational Axisymmetric Flows

H. R. GRISWOLD* AND A. L. MORRIS†
Pratt & Whitney Aircraft, East Hartford, Conn.

Introduction

IN recent years considerable attention has been given to axisymmetric flows especially in the design of turbomachinery. While numerical procedures for solving axisymmetric flow problems have been ingeniously developed,[1,2,3] it is often not possible to carry out a direct check on their accuracy. The object of the present Note is to present a family of simple exact solutions to the stream function equation for incompressible, irrotational, axisymmetric flow which have proven useful in testing the accuracy of numerical procedures associated with more general axisymmetric flows. These exact solutions are also of interest in that they correspond to certain fluid flow problems.

Analysis

The stream function equation for incompressible, irrotational, axisymmetric flow can be written in cylindrical coordinate form as:

$$\frac{\partial^2\Psi}{\partial r^2}-\frac{1}{r}\frac{\partial\Psi}{\partial r}+\frac{\partial^2\Psi}{\partial Z^2}=0 \tag{1}$$

where r, Z are the cylindrical coordinates in the radial and axial directions and $\Psi(r,z)$ the stream function. There are several obvious exact solutions to (1), for example $\Psi = Z$ or the trivial solution $\Psi = \text{const}$. There are other simple exact solutions. For any integer $N > 1$ and real number a_1, consider the family of polynomials

$$\Psi_N(r,z)=\sum_{j=1}^{P} a_j r^{2j} Z^{N-2j} \tag{2a}$$

where,

$$P=\frac{2N+(-1)^N-1}{4}=\begin{cases}(N/2), \text{ for } N \text{ even}\\(N-1)/2, \text{ for } N \text{ odd}\end{cases} \tag{2b}$$

and‡

$$a_j=a_1\prod_{i=1}^{j-1}\left[\frac{(2i-N)(N-2i-1)}{4i(i+1)}\right], \qquad j=2,3,\ldots,P \tag{2c}$$

It is easy to show that these polynomials satisfy Eq. (1). Taking appropriate derivatives of Eq. (2a), substituting into Eq. (1) and combining terms gives

$$\frac{\partial^2\Psi_N}{\partial r^2}-\frac{1}{r}\frac{\partial\Psi_N}{\partial r}+\frac{\partial^2\Psi_N}{\partial Z^2}=\sum_{i=1}^{P-1} r^{2i}Z^{N-2i-2}[4i(i+1)a_{i+1}-(2i-N)(N-2i-1)a_i] \tag{3}$$

Making use of Eq. (2c) in the bracketed expression in Eq. (3) yields

$$4i(i+1)a_{i+1}-(2i-N)(N-2i-1)a_i\equiv 0$$

so that Eq. (3) becomes

$$\frac{\partial^2\Psi_N}{\partial r^2}-\frac{1}{r}\frac{\partial\Psi_N}{\partial r}+\frac{\partial^2\Psi_N}{\partial Z^2}=0$$

Therefore Ψ_N defined by Eq. (2) represent a family of polynomial solutions to the stream function Eq. (1) for axisymmetric flow. The first few of these solutions, for convenient choices of a_1, are given in tabular form in Table 1.

Table 1 Exact polynomial solutions

N	Ψ_N
2	r^2
3	Zr^2
4	$r^2(4Z^2-r^2)$
5	$Zr^2(4Z^2-3r^2)$
6	$r^2(8Z^4-12r^2Z^2+r^4)$
7	$Zr^2(8Z^4-20Z^2r^2+5r^4)$
8	$r^2(64Z^6-240Z^4r^2+12Z^2r^4-5r^6)$
9	$Zr^2(64Z^6-336Z^4r^2+280Z^2r^4-35r^6)$

A study of these polynomial solutions indicates that these stream functions represent flow into axisymmetric annular wedges, the precise wedge pattern dependent upon the order N of the polynomial. Individual streamlines are found from the equation $\Psi_N = \text{const}$, for particular choices of the constant. A typical streamline pattern, corresponding to Ψ_7, is shown in Fig. 1. The streamlines through the origin (straight lines) which define the wedge patterns are found from $\Psi_N = 0$ with $r = mz$, which for the case $N = 7$ is just

$$\Psi_7 = m^2z^7(5m^4-20m^2+8)=0 \tag{4}$$

The roots of Eq. (4) provide the slopes m for these lines shown in Fig. 1, yielding $r = 0$, $z = 0$, $r = \pm[(20+4(15)^{1/2})/10]^{1/2}z$ and $r = \pm[(20-4(15)^{1/2})/10]^{1/2}z$.

Testing Numerical Procedures

The following example shows how these exact solutions may be used to test numerical procedures for axisymmetric flow. Since the stream function Eq. (1) is linear, any linear combination of solutions is also a solution. For example

$$\begin{aligned}\Psi &= b_1+b_2\Psi_2+b_3\Psi_3\\ &= b_1+b_2r^2+b_3zr^2\end{aligned} \tag{5}$$

satisfies Eq. (1). From the definition of the stream function in the meridional, $r-z$, plane, the radial and axial components of velocity are respectively

$$\begin{aligned}C_r &= -(1/r)(\partial\Psi/\partial z)\\ C_z &= (1/r)(\partial\Psi/\partial r)\end{aligned} \tag{6a}$$

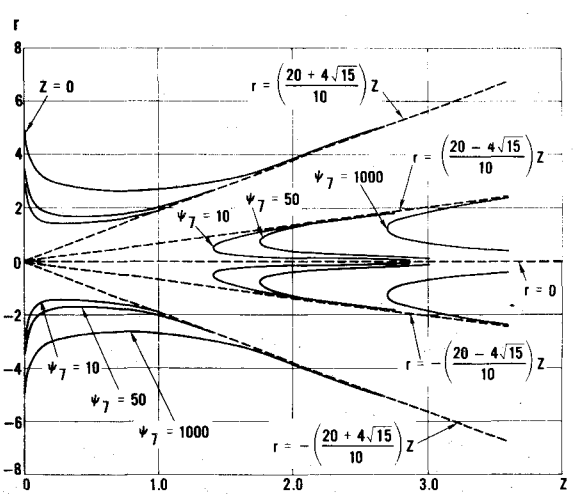

Fig. 1 Streamline pattern for seventh-order polynomial solutions, Ψ_7.

Received September 3, 1974; revision received October 16, 1974.
Index categories: Nozzle and Channel Flow; Computer Technology and Computer Simulation Techniques.

* Assistant Project Engineer, Compressor Research and Technology.
† Senior Analytical Engineer, Compressor Research and Technology. Member AIAA.

‡ The symbol Π is used to denote a product of terms.

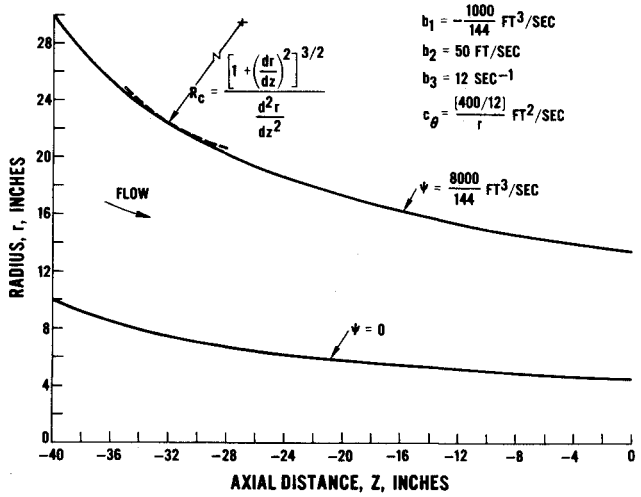

Fig. 2 Exact solution flowpath.

and the meridional velocity is just

$$C_M = (C_r^2 + C_z^2)^{1/2} \tag{6b}$$

These velocity components together with an axisymmetric irrotational choice of tangential velocity C_θ give, from Bernoulli's equation, the static pressure

$$P = P_T - \tfrac{1}{2}\rho(C_r^2 + C_z^2 + C_\theta^2)^{1/2} \tag{7}$$

for some choice of constant total pressure P_T and constant density ρ. Comparisons of the exact solution given in Eq. (5) with the results of two different numerical flow calculations is made in Figs. 2–5. One of the numerical calculations is based on a streamline curvature method,[3] and the other on a matrix through-flow method.[2] The flow path for this solution is the axisymmetric annular nozzle of Fig. 2. Exact solutions representing more complex flows can of course be found merely by choosing different combinations of polynomials. Static pressure, radius of curvature R_c and meridional velocity comparisons are made in Figs. 3–5. Note that the comparison shown in Fig. 4

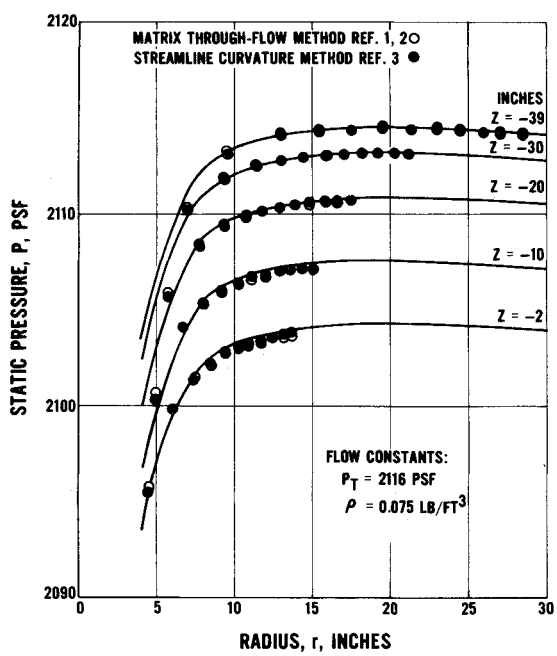

Fig. 3 Static pressures as calculated by computer programs compared with exact solution.

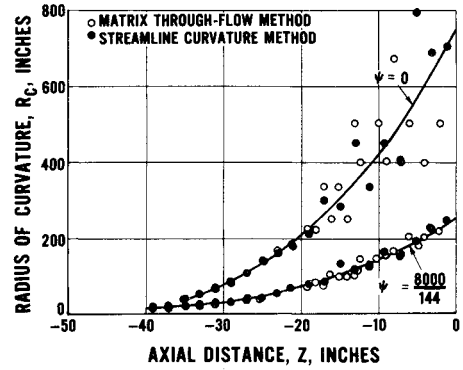

Fig. 4 Radii of curvatures as calculated by computer programs compared with exact solution.

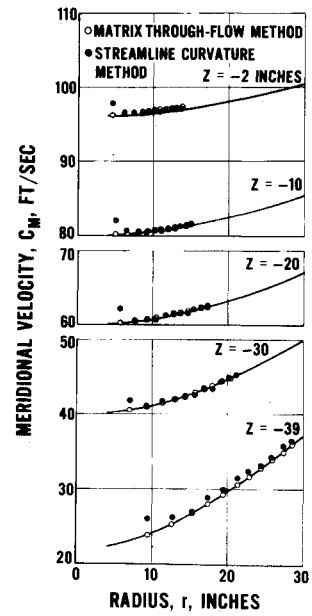

Fig. 5 Meridional velocities as calculated by computer programs compared with exact solution.

points out the sensitivity of the numerical calculation procedure of Ref. 3 to wall curvatures which, in turn, reflects in the rather poor agreement with the exact solution meridional velocities at the inner wall shown in Fig. 5. Herein lies the usefulness of the exact solution; that is, by making direct comparisons one can test not only the validity of the numerical calculation procedure but also determine if there is need to improve the accuracy of the scheme.

Conclusions

Testing the validity and accuracy of numerical procedures is greatly facilitated by the use of exact solution test cases when they are available. For the case of axisymmetric, irrotational, incompressible flow, a family of exact solutions have been presented, and one of these solutions was used to test two different calculation procedures for axisymmetric flow.

References

[1] Wu, C. H., "A General Theory of Three-Dimensional Flow in Subsonic and Supersonic Turbomachines of Axial, Radial, and Mixed-Flow Types," TN 2604, June 1952, NACA.

[2] Marsh, H., "The Through-Flow Analysis of Axial Flow Compressors," AGARD LS No. 39, Nov. 1970, Paris, France.
[3] Novak, R. A., "Streamline Curvature Computing Procedures for Fluid Flow Problems," ASME Paper 66-WA/GT-3, 1966.

Gardon Heat Gage Temperature Response

J. P. KITA* AND A. L. LAGANELLI†
General Electric Co., Valley Forge, Pa.

Nomenclature

ρ = density, #/ft^3
C_p = specific heat capacity, BTU/# m-°F
k = thermal conductivity, BTU/hr-ft-°F
$\mathscr{T}$ = thickness, in.
$\dot{q}$ = heat flux, BTU/hr-ft^2
T = temperature, °F
r = radius, inner, in.
t = time, sec
T_{ss} = steady state temperature, °F
R = radius, outer, in.
r^* = dimensionless radius ratio
T^* = dimensionless temperature ratio
t^* = dimensionless time ratio
$\overline{T}$ = transformed dimensionless temperature ratio
X = transformed dimensionless temperature ratio
A_j = Bessels coefficients
λ_j = eigenvalues
J_o = Bessels function, zero-order, first kind
J_1 = Bessels function, first-order, first kind
$\overline{T}_N$ = transformed dimensionless temperature ratio evaluated at the new boundary condition
T_{o_s} = initial temperature, °F

Introduction

ONE particular method of directly measuring the heat flux of a convective environment is through the use of a circular foil heat flux (Gardon) gage, whose basic operating principal is that the temperature difference between the center and edge of the foil face is directly proportional to the magnitude of the heat flux energy input to the gage. Inasmuch as the gage is generally calibrated in a controlled radiative environment with its edge temperature held constant, utilization of the gage in an environment where data are taken with a transient edge temperature, should be examined.

Gardon,[1] in originally describing the gage, solved the governing steady-state equation which basically states that incident heat flux is proportional to the foil center and edge temperature difference. The proportionality was found to be linear as a consequence of the fortuitous linear diffusivity of constantan. Gardon also proposed an approximate solution for the case of a uniform edge temperature in an effort to describe the speed of response of the gage. Later, Coffin[2] solved the uniform edge temperature problem for several varying heat flux inputs and addressed the problem of a varying sink temperature by stating that if the edge raises in temperature, the center temperature raises a proportional amount such that the gage output remains constant. An important result of the work of Laganelli and Martellucci[3,4] was that data taken from radiantly calibrated gages used in a convective environment, where test conditions dictated that the data be taken transiently with a rapidly varying edge temperature, agreed very well with data taken on identical models by several other independent and mutually supportive experimental techniques.

Received July 29, 1974; revision received October 7, 1974.
Index categories: Boundary Layers and Convective Heat Transfer—Turbulent; LV/M Aerodynamic Heating; Radiation and Radiative Heat Transfer.

* Systems Engineer, Environmental Power Operation.
† Consultant, Advanced Aerothermodynamics.

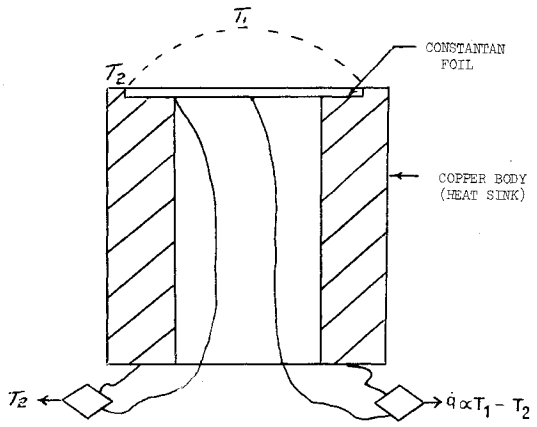

Fig. 1 Schematic of thin foil gage.

Analysis

Figure 1 is a schematic of a typical Gardon thin foil gage. The governing differential equation describing the temperature distribution for the circular foil gage is given by

$$\frac{\rho C_p}{k}\frac{\partial T}{\partial t} = \frac{\dot{q}}{\mathscr{T}k} + \frac{1}{r}\frac{\partial T}{\partial r} + \frac{\partial^2 T}{\partial r^2} \tag{1}$$

which is subject to the boundary conditions (zero edge reference temperature):

$$T(0,t) = \text{finite}; \quad T(0,\infty) = T_{o_s};$$
$$T(R,t) = 0; \quad T(r,0) = 0 \text{ (initially)}$$

The steady-state solution of Eq. (1), is

$$T_{ss} = T_{\text{center}} - T_{\text{edge}} = \dot{q}(R^2/4\mathscr{T}k) \tag{2}$$

That solution shows that heat flux is proportional to the steady-state temperature difference and was first applied to thin-foil heat gages by Gardon.

If the following dimensionless parameters are introduced

$$r = r^*R \tag{3a}$$
$$T = T^*T_{ss} \tag{3b}$$
$$t = t^*R^2/a \tag{3c}$$
$$a = k/\rho C_p \tag{3d}$$

Equation (1) is rewritten as

$$\frac{\rho C_p}{k} + \frac{\partial T^*}{\partial t^*}\frac{T_{ss}}{R^2}\frac{k}{\rho C_p} = \frac{\dot{q}}{\mathscr{T}k} + \frac{1}{r^*}\frac{\partial T^*}{\partial r^*}\frac{T_{ss}}{R} + \frac{\partial^2 T^*}{\partial r^{*2}}\frac{T_{ss}}{R^2} \tag{4}$$

Noting that

$$\dot{q}/\mathscr{T}k = 4(T_{ss}/R^2) \tag{5}$$

Equation (4) simplifies to

$$\frac{\partial T^*}{\partial t^*} = 4 + \frac{1}{r^*}\frac{\partial T^*}{\partial r^*} + \frac{\partial^2 T^*}{\partial r^{*2}} \tag{6}$$

If a linear transformation is applied to T such that

$$T^*(r^*,t^*) = \overline{T}(r^*,t^*) + X(r^*) \tag{7}$$

then the transformed boundary conditions become

$$\overline{T}(r^*=0,t^*) = \text{finite} \tag{8a}$$
$$\overline{T}(r^*=0,\infty) = 0 \tag{8b}$$
$$\overline{T}(r^*=1,t^*) = 0 \tag{8c}$$
$$\overline{T}(r^*,0) = 0 \tag{8d}$$